PROCEEDINGS OF SCIENCE

SANC: precision calculations for the SM processes

Dmitry Bardin[*] [†], *JINR, Dubna (Russia)*

E-mail: bardin@nusun.jinr.ru

Lidia Kalinovskaya [*] [†]

E-mail: kalinov@nusun.jinr.ru

Andrej Arbuzov [†]

E-mail: arbuzov@theor.jinr.ru

Serge Bondarenko [†]

E-mail: bondarenko@jinr.ru

Pena Christova [†]

E-mail: penchris@nusun.jinr.ru

Vladimir Kolesnikov [†]

E-mail: kolesnik@nusun.jinr.ru

Leonid Rumyantsev [†]

E-mail: leo_rumyantsev@inbox.ru

Renat Sadykov [†]

E-mail: srr@nusun.jinr.ru

Gizo Nanava, [‡], *IFJ, PAN (Poland)*

E-mail: Gizo.Nanava@ifj.edu.pl

We describe the present status of the computer system SANC (Support of Analytic and Numerical calculations for Colliders) v.1.10, intended for precision calculations of the event distributions for various decays and processes of the high energy elementary particle interactions in the NLO of the Standard Model (SM). At present, the system realises a semi-automatic chain of calculations from the SM Lagrangian up to a Monte Carlo (MC) event simulation for many $1 \to 2$ decays and $2 \to 2$ processes. Numerous comparisons with existing in the literature calculations are presented.

XI International Workshop on Advanced Computing and Analysis Techniques in Physics Research
April 23-27 2007
Amsterdam, the Netherlands

[*]Speaker.

[†]Supported in part by INTAS grant N^o 03-51-4007 and by Russian Foundation for Basic Research grant N^o 07-02-00932.

[‡]Supported by the EU grant mTkd-CT-2004-510126 in partnership with the CERN Physics Department and by the Polish Ministry of Scientific Research and Information Technology grant No 620/E-77/6.PRUE/DIE 188/2005-2008.

PoS(ACAT)077

1. Historical overview

The SANC project roots back to early 2001. It was announced first in Ref. [1] and its first phase status report was widely presented at ACAT2002 in several talks [2]–[5].

The main aim of the project is creation of a computer system for semi-automatic calculations of realistic and pseudo-observables for various processes of elementary particle interactions "from the SM Lagrangian to event distributions" at the one-loop precision level for the present and future colliders – TEVATRON, LHC, electron Linear Colliders (ISCLC, CLIC), muon factories etc.

Computer-wise, SANC is an IDE (Integrated Development Environment) and is realized as a server–client application. SANC client for version `v.1.10` can be downloaded from servers at CERN *http://pcphsanc.cern.ch/* and Dubna *http://sanc.jinr.ru/*.

Physics-wise, all the calculations at the one-loop precision level are realized in the spirit of the book [6] in the R_ξ gauge and all the results are reduced up to the scalar Passarino–Veltman functions: A_0, B_0, C_0, D_0. This two distinctive features allow to perform several checks: e.g. to test gauge invariance by observation the cancellation of gauge parameters dependence, to test various symmetry properties and validity of various Ward Identities, all at the level of analytical expressions. The process of calculation is structured into several well-defined steps. With the help of SANC system it is easy to follow all steps of calculations for many SM decays and processes. This makes the SANC system particularly appealing for educational purposes.

The SANC system uses several computer languages, but only FORM — for analytic calculations [7]. All the codes are put into a special program environment, written in JAVA. At early phase it was used for a revision of Atomic Parity Violation [8], for a calculation of the one-loop electroweak radiative corrections for the process $e^+e^- \to f\bar{f}$ [9] and neutrino DIS [10]. Meantime, in Ref. [11] it was used for precision comparison of EW corrections for the SM boson decays into fermion-antifermion pair and in [12] for an improvements of PHOTOS Monte Carlo generator.

In the second phase of the project (2004–2006), the calculations were extended to a large number of HEP processes, with an emphasis on LHC physics. In Ref. [13] we have summarized the status of the SANC version `1.00`, into which we implemented theoretical predictions for many high energy interactions of fundamental particles at the one-loop precision level for up to 4-particle processes. In this paper we placed an emphasis on an extensive discussion of the so-called "Pre-computation procedure", an important first step of calculations of the one-loop amplitudes for 3- and 4-particle processes in QED, QCD and EW theories. Finally, in Ref. [14] we described SANC version `1.10` upgraded both physics-wise and computer-wise compared to the version `1.00`. As far as physics is concerned it contains an upgraded treatment of $u\bar{d} \to l^+\nu_l$ and $d\bar{u} \to l^-\bar{\nu}_l$ processes used for precision calculations of Drell–Yan processes (see Ref. [15]) and a complete implementation of $t \to b + l^+ + \nu_l$ CC decays up to numbers and MC generators [16, 17]. We also implemented several processes like $f_1\bar{f}_1 ZZ \to 0$ and $f_1\bar{f}_1 HZ \to 0$, and the process $H \to f_1\bar{f}_1 A$ in three cross channels [18] in the EW branch, $\gamma\gamma \to \gamma\gamma$ scattering [19] and $l\,l \to \gamma\gamma^*$ in the QED branch, as well as a new QCD branch [20]. Starting from Ref. [14] we use a generalized approach: we begin with a presentation of the covariant amplitudes for a process, say $f_1\bar{f}_1 HZ \to 0$, where $\to 0$ means that all 4-momenta flow inwards. The derived scalar form factors can be used for any physically sensible cross channel (here two: annihilation $f_1\bar{f}_1 \to HZ$ and decay $H \to Z f_1\bar{f}_1$, since it is known that $M_H > M_Z$) after an appropriate permutation of their arguments (s,t,u). Then we compute helicity

amplitudes for every cross channel separately. Recently, in the same spirit we considered the three channels of the process $f_1\bar{f}_1 ZA \to 0$ [21].

In this report we will concentrate on recent studies results which have been published after 2005 or are being prepared for publication.

Whenever possible, we compare our results with those existing in the literature. For this comparison we widely used several well known codes or computer systems. At tree level we compared with GRACE-tree [22], CompHEP [23], PHOTOS [25]–[24], PYTHIA [26] whereas one-loop level results were checked against HORACE [27]–[29], WGRAD2 [30]–[31], ZGRAD2 [32]–[33], a code by S. Dittmaier and M. Kramer [34], FeynArts [35]–[38] and GRACE-loop [39].

2. Processes available in present version 1.10

The recent version of SANC deals with the three models of elementary particle interactions QED, EW and QCD. In the Fig. 1 we show processes only for EW branch.

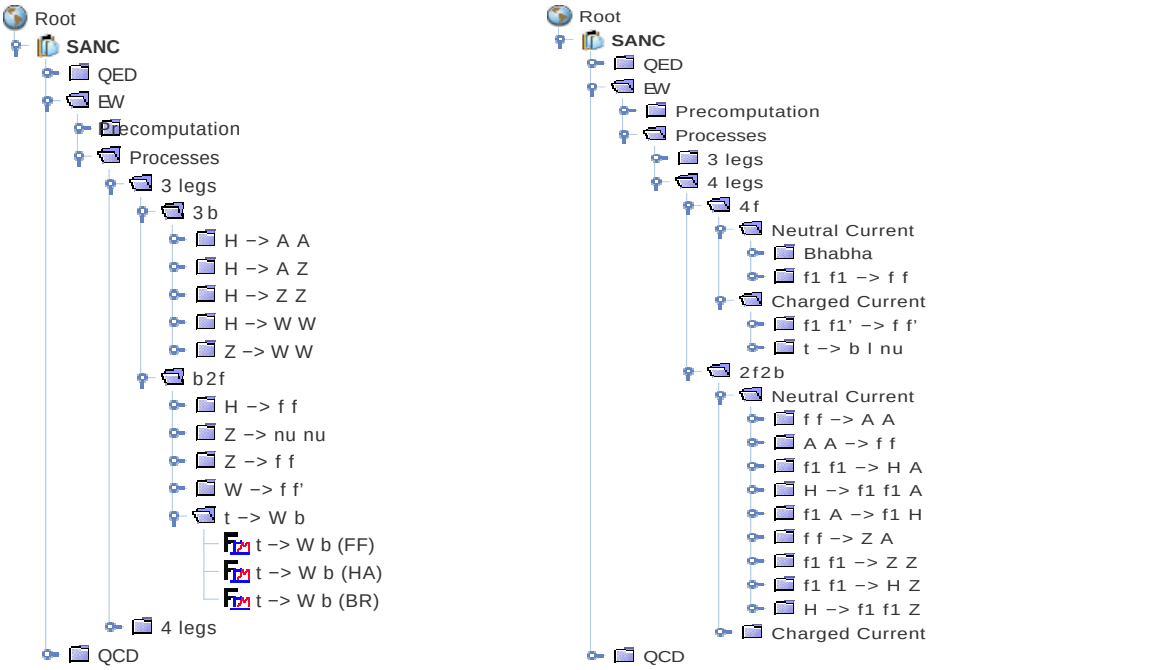

Figure 1: Three and four particle EW processes available in SANC version 1.10

Each tree consists of several levels of "folders" which end up with "files", normally three: FF (Form Factors), HA (Helicity Amplitudes) and BR (Bremsstrahlung). For labels of folders we use notations: b – for any boson; $f(f_1)$ – for any fermion (f_1 for massless fermions of the first generation whose mass is kept only in arguments of logarithmic functions); A,Z,W,H – for a photon, Z,W,H bosons; for files — the same but t,b, which mean here top and bottom quarks.

For many processes SANC calculations end up with MC integrators or event generators. But only few of them are embedded into the system itself, see Ref. [5] and Fig. 11 in Appendix. The other codes are accessible as the stand alone ones. The latter widely use FORTRAN modules generated by the system (see below).

2.1 Basic notions: precomputation, amplitudes, form factors...

Precomputation is one of important concept of SANC ideology. Since many one-loop calculations are enormously time consuming, the idea is to precompute as many one-loop diagrams and derived quantities (renormalization constants, etc) as possible. The precomputation trees are presented and exhaustively discussed in the Ref. [13] and we refer the reader to this paper.

As seen from an open folder for $t \to Wb$ decay in the Fig. 1, one has usually three files written in FORM, which compute:

- Covariant amplitude (CA) and scalar FF, cf. with the nucleon-nucleon-γ vertex parametrized by the two scalar FF $\mathscr{F}_{1,2}$: $\mathscr{A} \propto \gamma_\mu \mathscr{F}_1 + \sigma_{\mu\nu} q_\nu \mathscr{F}_2$;
- HA, which depend on FF, $\mathscr{H}_{\{\lambda_i\}}(\mathscr{F}_i)$, where $\{\lambda_i\}$ denotes a set of helicity quantum eigenvalues, typically spin projections onto a quantization axis. We remind that in the standard approach for an observable O one has: $O \propto |\mathscr{A}|^2$, while in terms of HA: $O \propto \sum_{\{\lambda_i\}} |\mathscr{H}_{\{\lambda_i\}}|^2$ and this drastically simplifies calculations since $\mathscr{H}_{\{\lambda_i\}}$ are scalar objects which are computed as complex numbers. Many other examples of CA and HA maybe found in Refs. [13], [14] and [18];
- Accompanying real BR. This module computes the contribution of the real bremsstrahlung to a relevant process. Typically we have both the calculations of inclusive quantities and fully differential ones for a use in the MC codes.

2.2 From analytic results to numbers

The chain of SANC calculations starts with on-line execution of module FF, followed by an s2n run (see short User Guide at our Project home pages, indicated in the Introduction), and subsequent execution of module HA with another s2n run. As the result, the system generates a FORTRAN code for the contribution of virtual corrections to a chosen process in the following schematic form:

$$d\Gamma(d\sigma) \sim \sum_{\lambda_i\lambda_j\lambda_k\lambda_l} \left| \mathscr{H}\left(\mathscr{F}^{\text{Born+1loop+2loop}}\right)_{\lambda_i\lambda_j\lambda_k\lambda_l} \right|^2 . \tag{2.1}$$

Note, that the 2-loop corrections may be easily embedded into this scheme if available.

Real corrections consists of Soft and Hard bremsstrahlung. They are computed by modules BR. The Soft has the Born-like kinematics, while Hard has + 1 particle's more phase space and typically the system creates a FORTRAN module which is used in subsequent MC calculations. For several processes, the system may compute complete one-loop corrections, including real bremsstrahlung for an inclusive observable.

For numerical computations we use the FORTRAN modules generated by the package s2n — a part of the system written in PERL. SANC includes its own FORTRAN library for numerical calculation of Passarino–Veltman functions and uses LoopTools as an alternative (see, [40]).

2.3 Types of SANC Outputs

So, typical SANC outputs are:

- FORTRAN modules.
  These modules may be used in MC integrators and generators by ourselves or by the others;
- Standalone MC generators.
  As example we will present below some result obtained with:
  a) generator for $t \to bl\nu$ decay;
  b) generators for NC and CC Drell–Yan processes;
  c) generator for $H \to 4\mu$ decay in the single Z pole approximation;
- Contribution to tuned comparison.
  It has an impact on competition of precision MC generators at the LHC era. So far we participated in two workshops: Les Houches Workshop, see Proceedings 2006 [42] and TEVATRON for LHC Report, 2007, [43].

3. SANC application for selected processes

In this section we present some recent results obtained with SANC for several selected processes:

- $t \to bl\nu$ decay;
- $\bar{f}_1 f_1 \to ZZ$;
- $\bar{f}_1 f_1 HA \to 0$: three cross channels;
- $\bar{f}_1 f_1 ZA \to 0$: three cross channels;
- $\bar{f}_1 f_1 HZ \to 0$: two cross channels;
- $H \to 4\mu$ decay;
- Drell–Yan-like W and Z production.

These results were published in 2006–2007 or are still in preparation.

3.1 $t \to bl\nu$ decay

The results of this study are published in Ref. [16, 17]. We presented there:

- total width and various distributions;
- calculated without and with one-loop EW and QCD corrections;
- results of complete calculations and of the pole approximation;
- results obtained with MC integrator and event generator;
- comparison with world literature.

As a typical result obtained with the MC event generator we show in Fig. 2 the complete EW correction $\delta = (d\Gamma^{1\text{loop}}/dM_{l\nu_l})/(d\Gamma^{\text{Born}}/dM_{l\nu_l}) - 1, \%$ as a function of invariant mass of $M = M_{l\nu_l}$ pair.

As seen from the Fig. 2, EW correction is very big below the resonance and rather small at and above resonance.

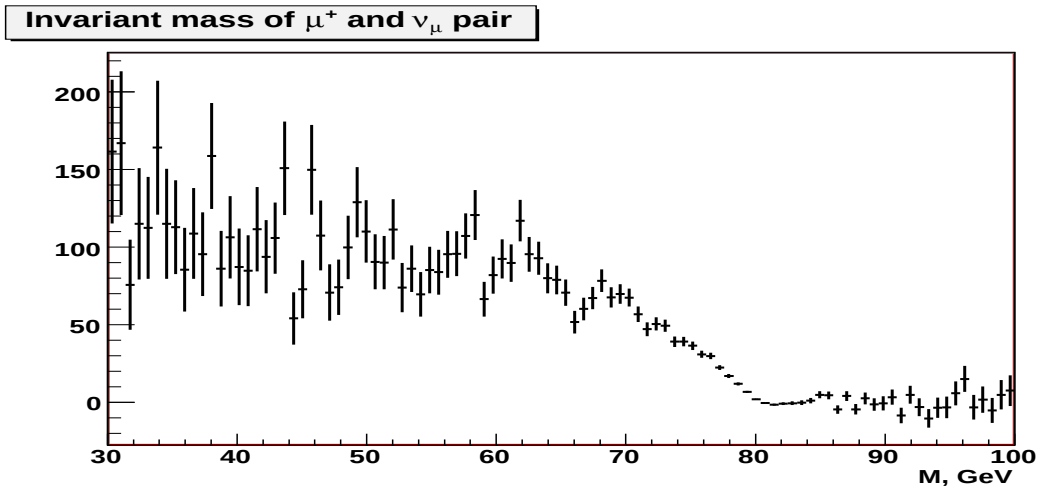

Figure 2: Complete EW correction δ (in %) as function of invariant mass of lepton pair $M_{l\nu_l}$

3.2 $f_1\bar{f}_1 \to ZZ$

In Ref. [14] we presented our analytic results for one-loop EW corrections for the process $f_1\bar{f}_1 \to ZZ$, however, we did not manage to perform the numerical comparison with results of Ref. [49] because of a misinterpretation of some statements of this paper. Recently we came back to this point and found an excellent agreement with their numbers of fourth column from their Table 1 ($M_H = 100$ GeV) as seen from the Table 1.

$\sqrt{s}$, GeV	θ	[49] δ,%	SANC δ,%
190	10°	16.13	16.134
	45°	16.22	16.225
	90°	16.32	16.321
210	10°	13.88	13.879
	45°	13.93	13.932
	90°	13.85	13.849
250	10°	12.64	12.642
	45°	11.96	11.959
	90°	10.47	10.473
500	10°	13.26	13.258
	45°	5.51	5.514
	90°	-1.68	-1.679
1000	10°	11.89	11.888
	45°	6.00	-6.000
	90°	-17.66	-17.660

Table 1: Comparison of the weak 1-loop correction δ in % for the $e^+e^- \to ZZ$ process (input as in Ref. [49]).

In SANC we also have the hard photons contribution and the possibility to compute the hadron level process: $pp \to ZZ$.

3.3 Three channels of $f_1\bar{f}_1 HA \to 0$

In a recent Ref. [18] we present the results of a unified approach when we begin with a common CA of all cross channels of process $f_1\bar{f}_1 HA \to 0$, in which 4-momenta of external particles are incoming:

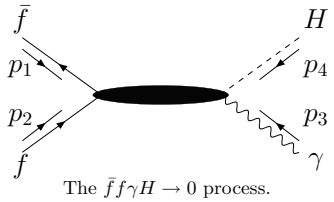

The $\bar{f}f\gamma H \to 0$ process.

For $f_1\bar{f}_1 HA \to 0$ processes, the CA at one-loop order has the form:

$$\mathscr{A}^{\text{Born+1-loop}} = \mathscr{A}^{\text{Born}}[\mathscr{O}(m_f^2)] + \mathscr{A}^{\text{1-loop}}[\mathscr{O}(\alpha)] + \mathscr{A}^{\text{1-loop}}[\mathscr{O}(m_f^2\alpha)]\,. \tag{3.1}$$

The second term, $\mathscr{A}^{\text{1-loop}}[\mathscr{O}(\alpha)]$, stands for a part of one-loop amplitude not suppressed by Yukawa coupling (m_f^2) contrary to the Born amplitude $\mathscr{A}^{\text{Born}}[\mathscr{O}(m_f^2)]$ and to the rest of one-loop amplitude $\mathscr{A}^{\text{1-loop}}[\mathscr{O}(m_f^2\alpha)]$.

For this reason Born amplitude typically contribute less than the one-loop one and the squared amplitude becomes:

$$|\mathscr{A}^{\text{Born+1-loop}}|^2 \longrightarrow |\mathscr{A}^{\text{Born}}[\mathscr{O}(m_f^2)] + \mathscr{A}^{\text{1-loop}}[\mathscr{O}(\alpha)]|^2. \tag{3.2}$$

For the first generation fermions even $\mathscr{A}^{\text{Born}}$ could be neglected, but it can be significant for the second and third generations. The QED one-loop and the bremsstrahlung corrections contribute to the third term of Eq.(3.1), so they could be also neglected.

Then SANC computes the analytical expressions of the HA for all three channels separately making an appropriate permutation of incoming momenta and projecting CA to the states with definite helicities. Three cross channels of the process $f_1\bar{f}_1 HA \to 0$ and the momenta flow of particles involved are schematically given in Fig. 3. HA for all three channels are presented in

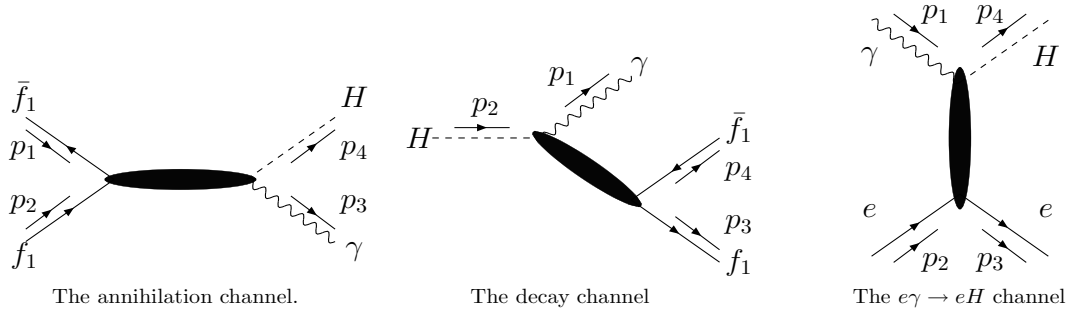

Figure 3: Three and four particle EW processes available in SANC version 1.10

Ref. [18]. Here we give only some numerical results for every channel.

3.3.1 Annihilation channel $f_1\bar{f}_1 \to HA$

The Fig. 4 shows one-loop corrected cross section of the Higgs boson production via annihilation process as a function of the Higgs boson mass, M_H in the same style as Fig. 2 of Ref. [44].

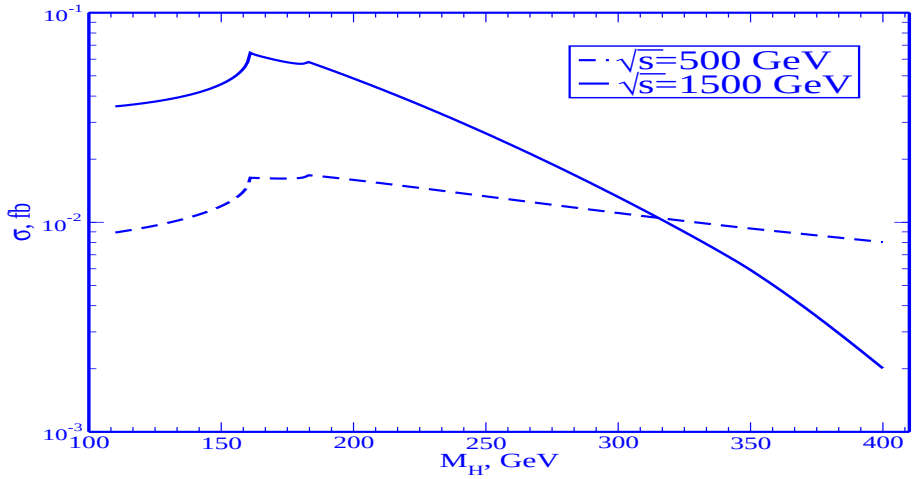

Figure 4: Completely EW corrected σ in fb, as function of the Higgs boson mass

Though we did not manage to perform a "tuned" comparison of our results, there is a good "visual" agreement with Fig. 2 of Ref. [44].

3.3.2 Decay channel $H \to \mu^+\mu^-\gamma$

For the decay channel we did not find a reference whom to compare with. In the Fig. 5 we show the $M_{\mu^+\mu^-}$ invariant mass distribution at the Born and one-loop levels for $M_H = 150$GeV.

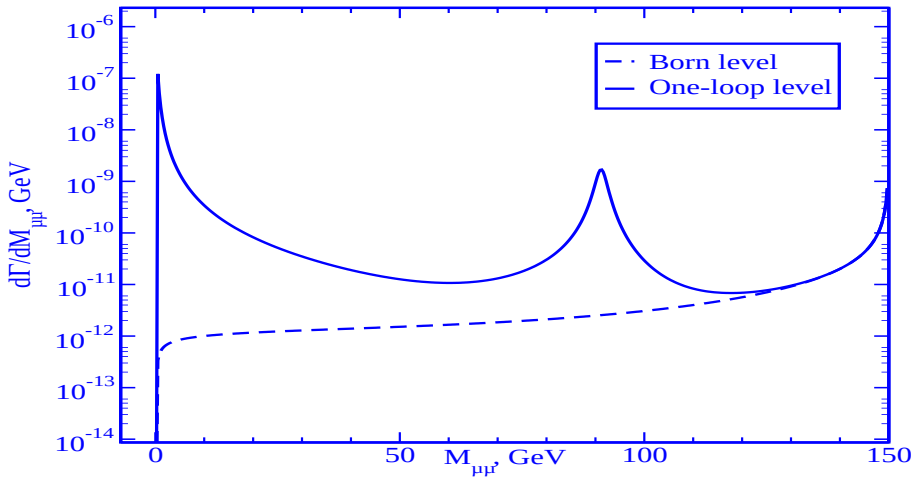

Figure 5: Invariant mass distribution, Born (dashed) and one-loop levels (solid line)

The two peaks due to γ and Z exchanges are distinctly seen. The Born contribution is small everywhere except for the soft photon corner, where it develops an infrared divergence. More numerical results are presented in Ref. [18].

3.3.3 The production channel $e\gamma \to eH$

For this channel, we present an almost tuned comparison between the results shown in Table I of Ref. [45] and SANC for three cms energies $\sqrt{s} = 500,\ 1000,\ 1500$ GeV and wide range of Higgs mass: 110 GeV$\leq M_H \leq$ 400 GeV.

$M_H/\sqrt{s}$	500			1000			1500		
	SANC	[45]	δ	SANC	[45]	δ	SANC	[45]	δ
80	8.40	8.38	-0.2	9.31	9.29	-0.2	9.76	9.74	-0.2
100	8.85	8.85	0	9.95	9.94	-0.1	10.48	10.5	-0.2
120	9.77	9.80	0.3	11.16	11.2	0.4	11.80	11.8	0
140	11.76	11.8	0.3	13.68	13.7	0.1	14.52	14.6	0.6
160	20.91	21.1	0.9	24.82	25.0	0.7	26.48	26.6	0.5
180	20.67	20.9	1.1	25.04	25.3	1.0	26.81	27.0	0.7
200	16.99	17.2	1.2	21.05	21.2	0.7	22.64	22.8	0.7
300	5.90	5.97	1.2	8.44	8.53	1.0	9.33	9.43	1.1
400	1.64	1.64	0	2.74	2.78	1.5	3.15	3.18	1.0

Table 2: Total cross sections σ in pb and relative difference δ in % between SANC and Ref. [45].

In the Table 2 we show total cross sections σ and relative difference δ between the two calculations ($\delta = \sigma[45]/\sigma[\texttt{SANC}] - 1$, (%)). As seen, the difference in many of points is below 1% and shows up an irregular behavior pointing to its numerical origin (our numbers are calculated with real*16). We consider the two results to be in a very good agreement.

3.4 Three channels of $f_1\bar{f}_1 ZA \to 0$

Recently we implemented another three cross channels of $f_1\bar{f}_1 ZA \to 0$: annihilation, $f_1\bar{f}_1 \to ZA$; decay, $Z \to f_1\bar{f}_1 A$, and production, $e\gamma \to eZ$.

$\sqrt{s}$, GeV	θ		DD [46]	Grace-loop [39]	SANC [21]
500	$20^\circ < \theta < 160^\circ$	$\sigma^{\rm Born}$, pb	0.7051	0.70515	0.70515
		δ, %	-25.69	-25.689	-25.690
	$1^\circ < \theta < 179^\circ$	$\sigma^{\rm Born}$, pb	1.770	1.7696	1.7697
		δ, %	-22.31	-22.313	-22.313
2000	$20^\circ < \theta < 160^\circ$	$\sigma^{\rm Born}$, pb	0.04620	0.046201	0.046201
		δ, %	-39.53	-39.529	-39.529
	$1^\circ < \theta < 179^\circ$	$\sigma^{\rm Born}$, pb	0.1170	0.1170	0.11697
		δ, %	-30.84	-30.845	-30.845

Table 3: Comparison of the Born cross section pb and δ in % of the $\gamma e^- \to Ze^-(\gamma)$ reaction ([DD] input and $E_\gamma \leq 0.025\sqrt{s}$ GeV).

For every channel SANC generates the corresponding hard photon emission contribution [21]. We found a paper whom to compare with by A. Denner and S. Dittmaier (DD) [46]. In Table 3 we

show only a part of their Table 5.3 where we also added Grace-loop numbers taken from Ref. [39]. As seen, there is perfect agreement between three calculations with the same input.

3.5 Two channels of $\bar{f}_1 f_1 HZ \to 0$

The calculations of this process in two channels: annihilation $\bar{f}_1 f_1 \to HZ$ and decay $H \to Z\bar{f}_1 f_1$ are presented in Ref. [14]. Here we present only its CA and several numerical results.

3.5.1 Covariant amplitude of the process

The reason of presenting CA for this process is its compactness, it is described by 6 structures and 6 form factors. Introducing all incoming momenta as $\bar{f}_1(p_1) f_1(p_2) Z(p_3) H(p_4) \to 0$, one has:

$$\mathscr{A}_{ffHZ} = k\Big\{ \Big[\bar{v}(p_1)\big(\gamma_\nu\gamma_+\sigma_f \mathscr{F}_0^+(s,t) - \not{p}_3\gamma_+(p_1)_\nu \mathscr{F}_1^+(s,t) - \not{p}_3\gamma_+(p_2)_\nu \mathscr{F}_2^+(s,t)\big)u(p_2)\,\varepsilon_\nu^Z(p_3)\Big] + \Big[\sigma_f \to \delta_f,\ \gamma_+ \to \gamma_-\ \mathscr{F}_i^+(s,t) \to \mathscr{F}_i^-(s,t)\Big]\Big\}, \tag{3.3}$$

where

$$\gamma_\pm = 1 \pm \gamma_5, \quad \sigma_f = v_f + a_f, \quad \delta_f = v_f - a_f, \quad k = -\frac{ig^2}{4c_W^2}\frac{M_Z}{M_Z^2 - s}. \tag{3.4}$$

3.5.2 Annihilation channel $e^+e^- \to HZ$

For the annihilation channel we present the results of a triple comparison, see Table 4: Again,

$\sqrt{s}$, GeV	M_H, GeV	Grace-Loop [39]	[41]	SANC [14]
500	100	4.1524	4.1524	4.1524
500	300	6.9017	6.9017	6.9017
1000	100	−2.1656	−2.1656	−2.1656
1000	300	−2.4995	−2.4995	−2.4995
1000	800	26.1094	26.1094	26.1094
2000	100	−11.5413	−11.5414	−11.5414
2000	300	−12.8226	−12.8226	−12.8226
2000	800	11.2468	11.2468	11.2468

Table 4: EW corrections to the total cross section in percent in α scheme.

one observes an excellent agreement between three calculations. In SANC we implemented also complete NLO EW corrections, including hard photon bremsstrahlung.

3.5.3 Decay channel $H \to Z f_1 \bar{f}_1(\gamma)$

For the decay channel we did not found a paper whom to compare with. In Fig. 6 we show distributions over invariant mass $m^2_{\mu^+\mu^-(\gamma)}$. A narrow peak at low mass is distinctly seen. It has simple physical explanation. Since the $H \to Z\gamma$ width does not vanish for an on-shell photon with $Q^2_\gamma = 0$, the one-loop amplitude for $H \to Z f_1 \bar{f}_1$ with virtual photon exchange will show a $\sim 1/s$ behavior (with $s = -Q^2_\gamma$). This, in turn, will lead to the $\sim 1/s$ behavior of both the double and

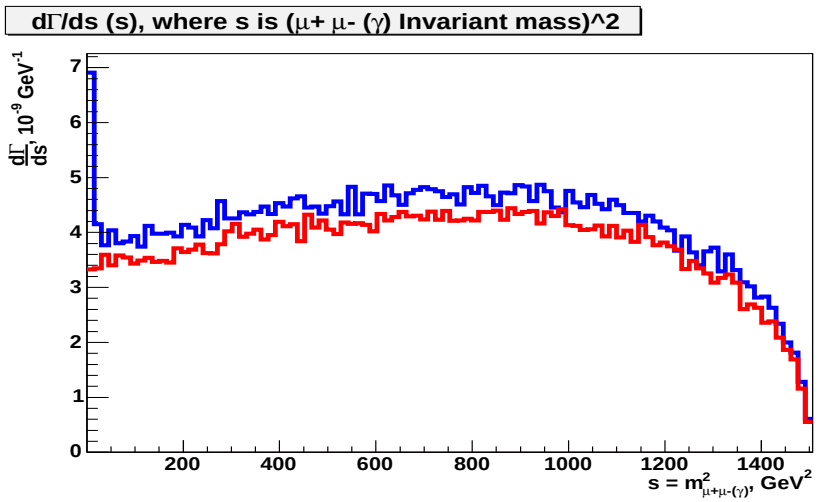

Figure 6: The distributions over invariant mass $m^2_{\mu^+\mu^-(\gamma)}$ in α scheme. The red line shows Born level distribution while blue line — Born+1loop.

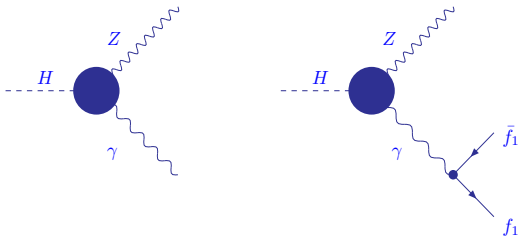

Figure 7: $H \to Z\gamma$ decay and Coulomb singularity

single differential widths. The $1/s$ region is very narrow and is largely washed out not only by a soft cut on the variable s but even by the plain s-integration.

For demonstration we prepare some benchmarks. For the $H \to Z f_1 \bar{f}_1$ decay see Benchmark case 3: Fig. 13 and Table 8 in Appendix.

3.5.4 $H \to Z f_1 \bar{f}_1$: a MC generator for $H \to 4\mu$ decay

Based on results of previous section, we developed a simple MC event generator which takes

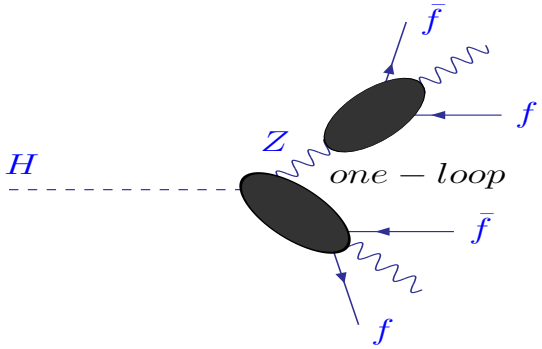

Figure 8: $H \to 4\mu$ in the single resonance approximation.

into account: identity of muons, one photon radiation and one-loop EW virtual corrections in the resonance approximation. The idea of this approach is illustrated in Fig. 8 and is described in more details in Ref. [14]. As was shown in [14], this approximation is valid for $130 \leq M_H \leq 160$ GeV. This event generator was transferred for use to JINR ATLAS muon group.

3.5.5 MC $H \to 4\mu$: Prophecy4f & SANC comparison

Recently there appeared a MC generator Prophecy4f based on a complete 5-point one-loop calculations Refs. [42, 50, 51]. We present a Table of comparison for partial width for decay $H \to 4\mu$ in G_μ scheme for $M_H = 140$ GeV between Prophecy4f and SANC.

M_H, GeV	120	130	140	150	160
Prophecy4f	0.7053(3)	2.3769(9)	6.692(2)	16.807(6)	40.06(1)
SANC (G_μ)	0.7197(3)	2.4079(8)	6.743(2)	16.842(5)	39.62(2)
δ,%	2.04	1.01	0.76	0.21	-1.10
SANC (α)	0.6938(2)	2.343(1)	6.594(2)	16.534(5)	39.15(1)

Table 5: Comparison for partial width in 10^{-7} GeV for decay $H \to 4\mu$ in G_μ scheme for $M_H = 140$ GeV between Prophecy4f and SANC

As seen from the Table 3.5.5, there is $\pm 1\%$ agreement in the mass range 130–140 GeV, degrading at the edges of the interval [120–160] as expected, see Ref. [14]. Note, that Prophecy4f uses another renormalization scheme and takes into account several higher order effects and that SANC calculations in α and G_μ schemes differ by about 2%.

The SANC generator was used for a MC simulation of $H \to 4\mu$ decay in the ATLAS detector and the results were compared with those obtained by PYTHIA, showing notable deviations, see [52]. This demonstrates the importance of higher order corrections and the necessity to reduce the theoretical error.

3.6 Drell–Yan-like W and Z production

The description of Drell–Yan-like single W and Z production processes are rather advanced in SANC. As usual, we begin with partonic level calculations by running relevant FF/HA/BR files each by FORM and s2n. The results of this run for CC Drell–Yan process are shown in Appendix, see Benchmark case 2: Fig. 12 and Table 7.

3.6.1 CC and NC Drell–Yan processes distributions

The FORTRAN modules, generated by s2n package, are used in MC integrators and generators based on Vegas algorithm. With the aid of the integrators we have produced numerous distributions presented in proceeding of Les Houches [42] and TeV4LHC [43] Workshops. Here we present a few distributions, both for CC and NC cases. The results obtained with the aid of generators will be presented elsewhere.

First of all, one has to introduce some notions.

- Charged current Drell–Yan (CC DY) production:
  - $q\bar{q}'$ sub-process
    $p[q]+p[\bar{q}']\to W^{\pm}\to X+\ell^{\pm}+\nu_{\ell}(+\gamma)$
  - gq sub-process
    $p[g]+p[q]\to W^{\pm}\to X+\ell^{\pm}+\nu_{\ell}(+g)$
  - γq or γ-induced sub-process
    $p[\gamma]+p[q]\to W^{\pm}\to X+\ell^{\pm}+\nu_{\ell}(+\gamma)$, $(\ell=e,\mu)$
- Neutral current Drell–Yan (NC DY) production:
  - $q\bar{q}$ sub-process
    $p[q]+p[\bar{q}]\to \gamma,Z\to X+\ell^{+}+\ell^{-}(+\gamma)$
  - gq sub-process
    $p[g]+p[q]\to \gamma,Z\to X+\ell^{+}+\ell^{-}(+g)$
  - γq or γ-induced sub-process
    $p[\gamma]+p[q]\to \gamma,Z\to X+\ell^{+}+\ell^{-}(+\gamma)$, $(\ell=e,\mu)$

For CC we computed $2\otimes 2\otimes 2$ distributions:

$$\begin{pmatrix} q\bar{q}' \\ g(\gamma)q \end{pmatrix}\otimes\begin{pmatrix} p_T \\ M_T \end{pmatrix}\otimes\begin{pmatrix} \mu \\ e \end{pmatrix}$$

In the first column the partons participating a hard sub-process are shown. In the second column — the variable of distribution: transverse leptonic momentum $p_T=p_T^{\ell}$ or transverse mass $M_T=\sqrt{2p_T^{\ell}p_T^{\nu}(1-\cos\varphi_{\ell\nu})}$ of $\ell\nu_{\ell}$ system. In the third column — the type of final charge lepton μ or e. Moreover, for muons we use the so-called "bare" setup and for electrons — "calo" set up with some e–γ recombination, see above mentioned Proceedings.

For NC case only middle column has different and obvious meaning.

$$\begin{pmatrix} q\bar{q} \\ g(\gamma)q \end{pmatrix}\otimes\begin{pmatrix} p_T \\ M_{\ell^+\ell^-} \end{pmatrix}\otimes\begin{pmatrix} \mu \\ e \end{pmatrix}$$

For initial parton$=\gamma$ we finished a recent paper [47]. We have also distributions with initial parton$=$ *gluon*, but they are still preliminary and we will not show them in this report.

The distributions are produced for the cross-sections σ (pb) and the relative corrections δ (%) where the last is defined by $\delta=\sigma^{1-\mathrm{loop}}/\sigma^{\mathrm{Born}}-1$ for NLO QCD and EW corrections originating from the $q\bar{q}'$ sub-process and by $\delta=\sigma^{\mathrm{g(\gamma)q}}/\sigma^{\mathrm{Born}}$ for corrections originating from the gluon (photon) induced processes.

We begin with two distributions for CC DY.

CC DY: σ, M_T distribution

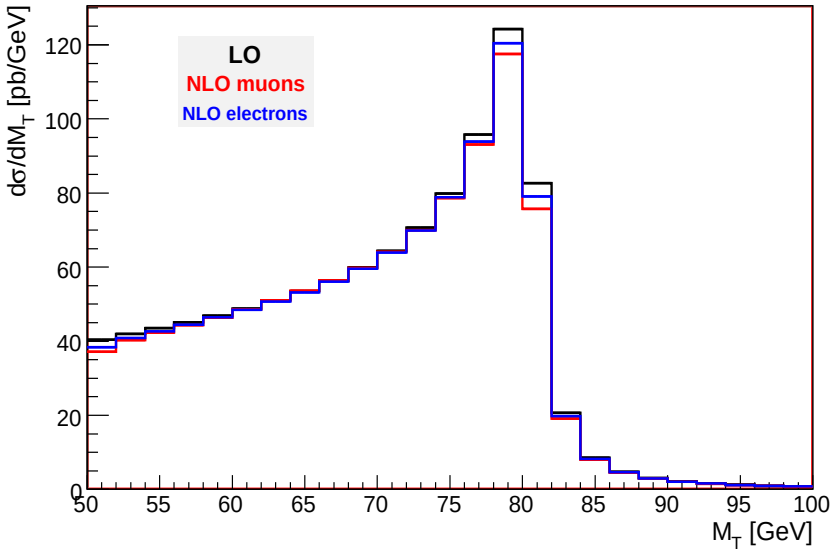

CC DY: δ, M_T distribution

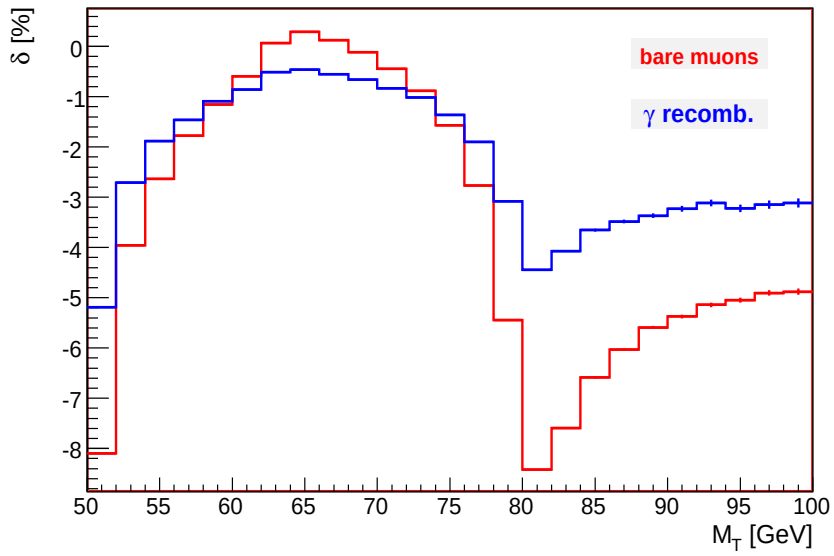

The EW correction is lower for the electrons due to recombination with photons.

The following two figures illustrate the contribution of γ-induced processes.

CC DY: δ, P_T^ℓ distribution

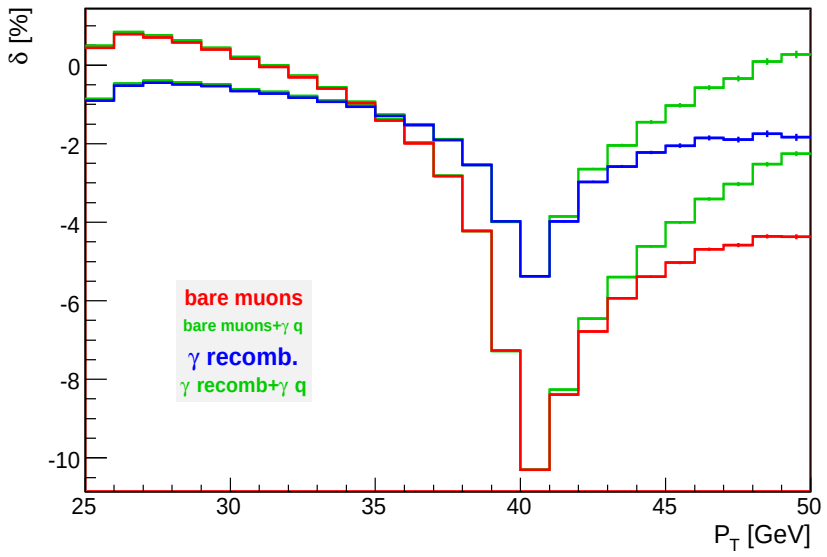

CC DY: δ, M_T distribution

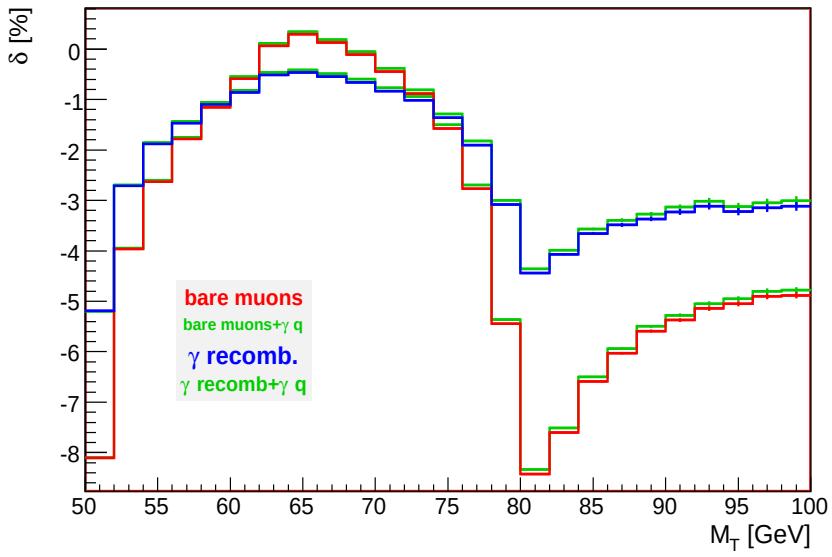

As seen, they are quite prominent in P_T^ℓ distribution and barely visible in M_T distribution.

Here we show only two distributions for NC DY.

NC DY: σ, $M_{\ell^+\ell^-}$ distribution

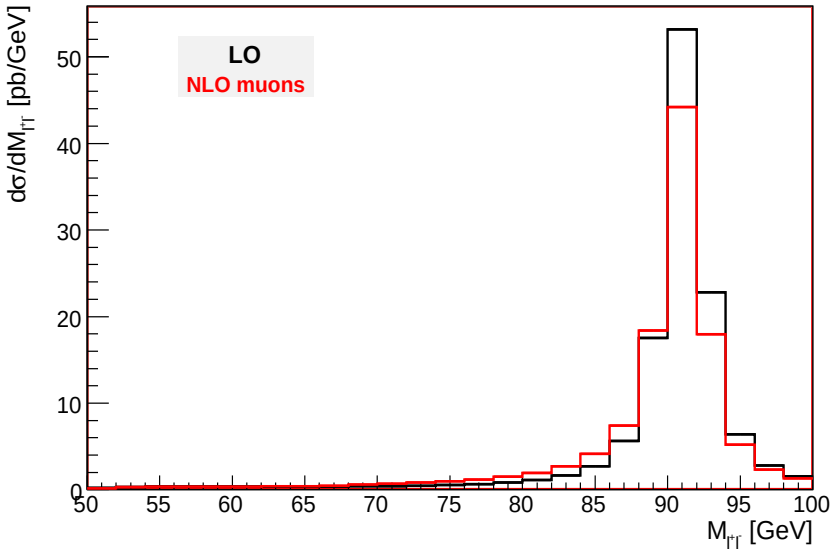

NC DY: δ, $M_{\ell^+\ell^-}$ distribution

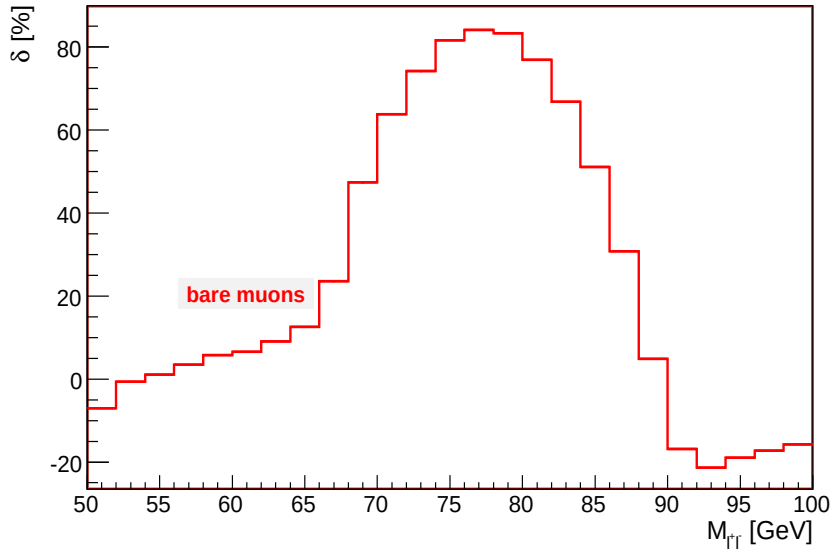

It is worth emphasizing that within two above mentioned Workshops, groups of participants dealing with DY processes did not manage to organize any “tuned comparison” for NC DY.

3.6.2 QCD-EW interplay

One of the most interesting questions in connection with Drell–Yan processes is the interplay of EW and QCD corrections at least in the NLO approximation. With the aid of SANC it is possible since we implemented NLO QCD correction exactly in the same language as we did for EW ones.

CC DY: δ, M_T distribution

QCD **EW**

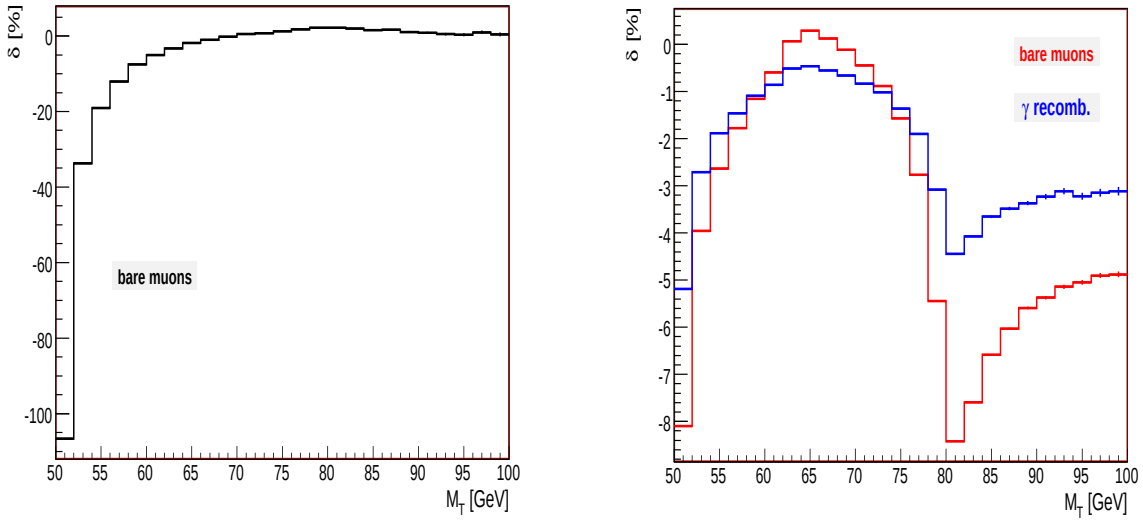

NC DY: δ, $M_{\ell^+\ell^-}$ distribution

QCD **EW**

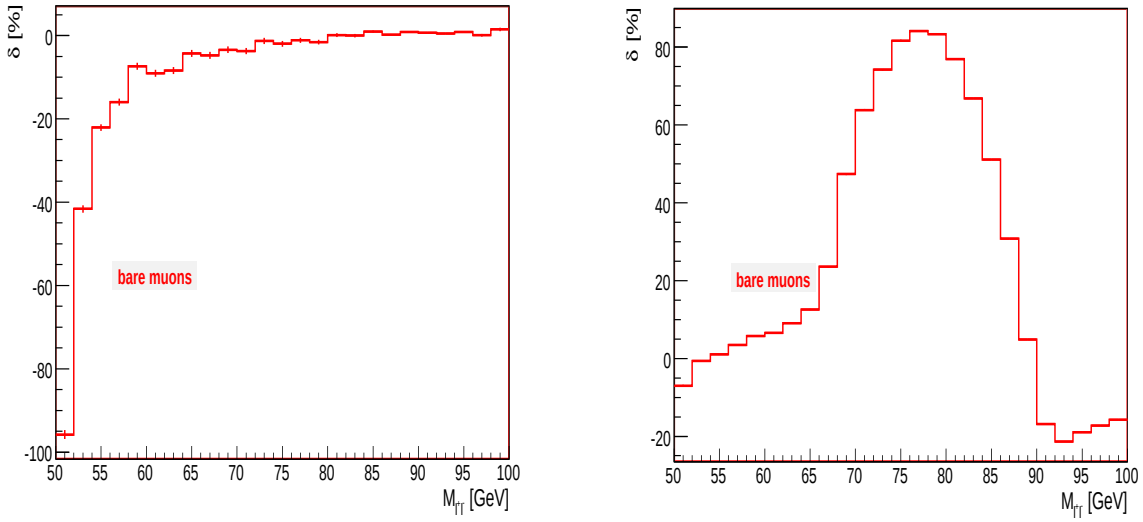

From these figures one may conclude that at least for some distributions NLO QCD corrections do not dominate. A more detailed presentation of this issue may be found in our reports to ATLAS MC working group [48]. (The upper left figure was statistically improved as compared to this report).

3.6.3 Drell–Yan processes: tuned comparison

The tuned comparison of EW corrections for CC Drell–Yan processes was started within the Les Houches Workshop [42], however, much more detailed study was performed within the TEV4LHC Workshop [43].

Three teams participated within TEV4LHC Workshop:

- `HORACE` — C.C. Calame, G. Montagna, O. Nicrosini, A. Vicini (Pavia, Italy) [27]–[29].
- `SANC` — SANC group (JINR, Dubna, Russia) [13]–[15].
- `W(Z)GRAD2` — U. Baur, D. Wackeroth (FNAL, USA) [30]-[33].

An example of tuned triple comparison within TEV4LHC workshop [43]

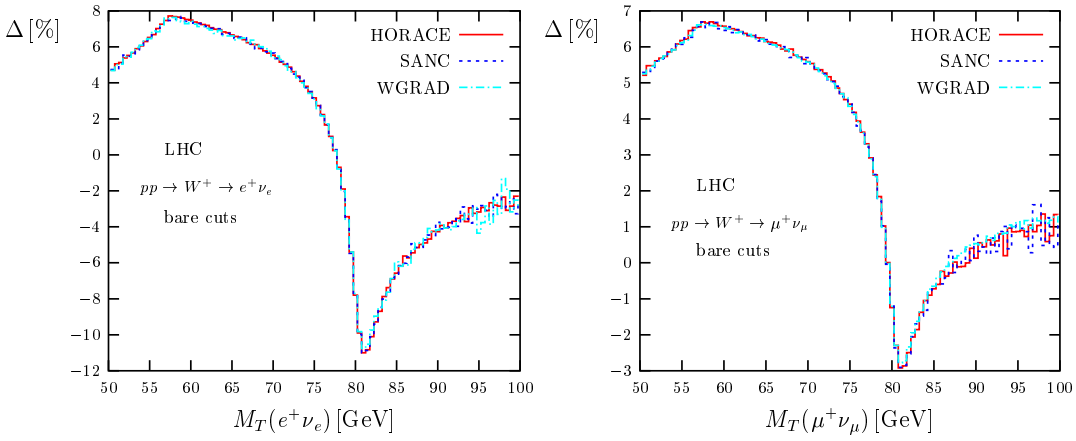

Figure 9: The relative correction Δ due to electroweak $\mathcal{O}(\alpha)$ corrections to the M_T distribution for single W^+ production with bare cuts at the LHC.

This figure illustrates that the issue of "technical precision" of EW NLO corrections for CC DY is well under control.

Appendix

As a part of our talk to ACAT2007, we gave an on-line demonstration of the SANC system. Here we have to limit ourselves by a presentation of several screen-shots corresponding to three benchmark cases described in the User Guides in Refs. [13], [14] (see also a joint User Guide in our Project home pages).

•Benchmark case 1: $\Gamma(Z \to b\bar{b})$ decay

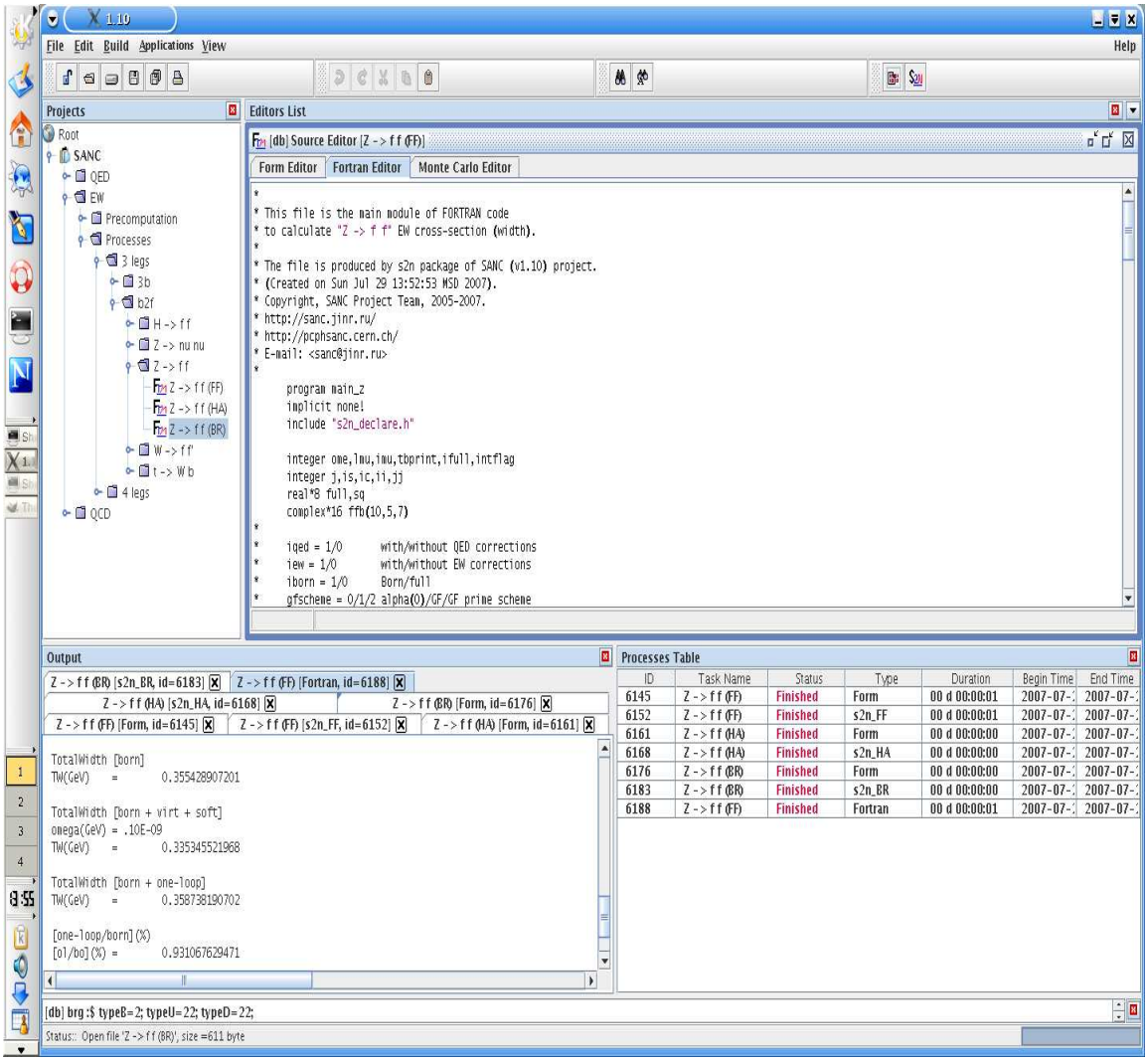

Figure 10: Working status of the SANC windows at the end of on-line calculations for $Z \to b\bar{b}$ decay: the first window (the left top corner) – the SANC tree, second (the right top corner) – the editor list window, third (the left bottom corner) – the output window with results for total widths for $Z \to b\bar{b}$ decay, and subsidiary window – the window of status processes (the right bottom corner). One can see 3 couples of FORM/s2n runs for FF/HA/BR, followed by a FORTRAN run to produce benchmark case 1 numbers, see also the Table 6.

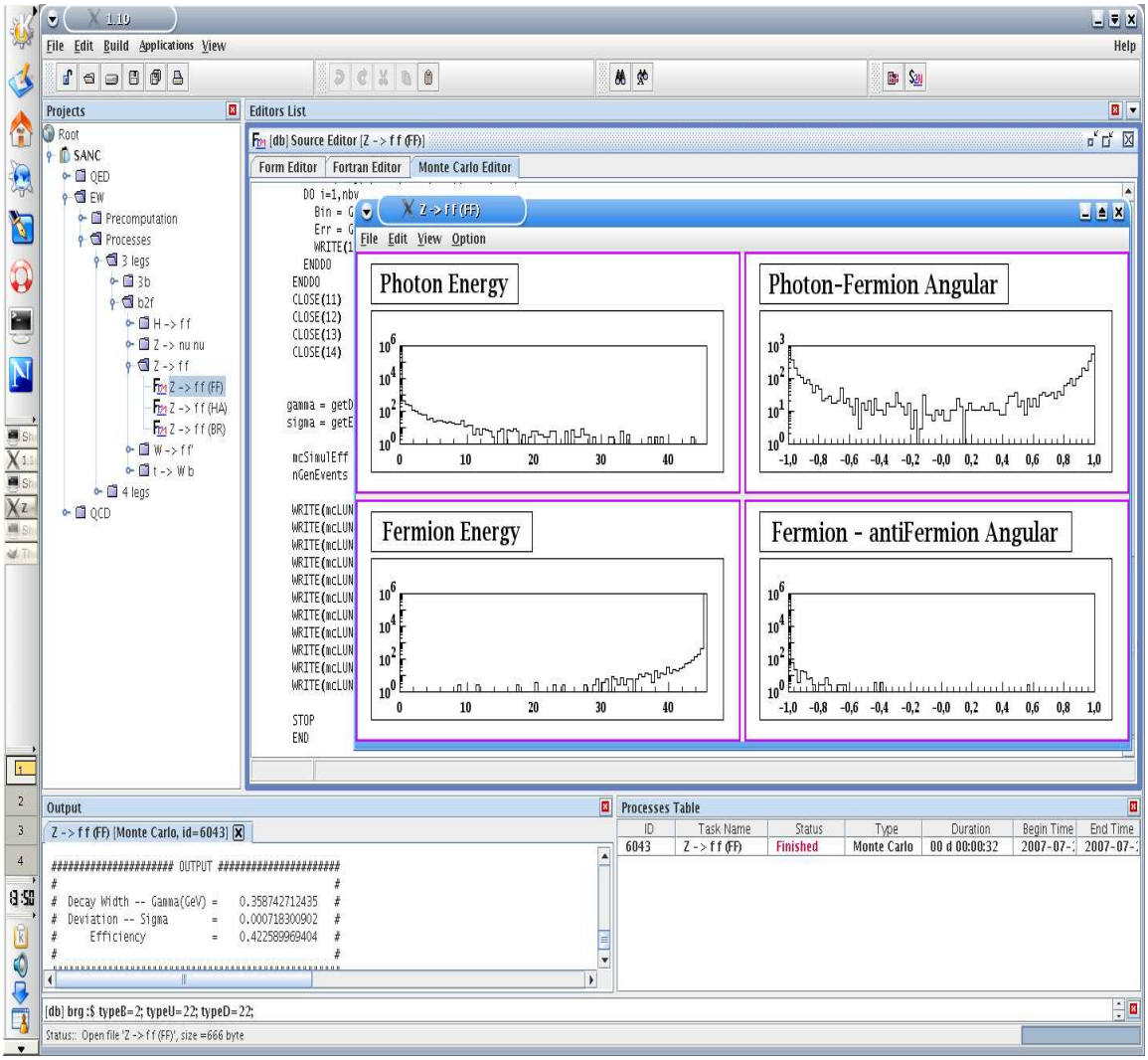

Figure 11: Working status of the SANC windows for $Z \to b\bar{b}$ decay at the end of on-line MC calculations. In the output window one sees the partial $Z \to b\bar{b}$ decay rate in GeV with its statistical MC error. One sees also four pre-defined histograms, which are requested by checking of four corresponding boxes at the Numerical form in the MC mode.

	Γ_{Born}	$\Gamma_{\text{Born+virt+soft}}$	Γ_{Total}
Semi-Analytic	0.355428	0.335345	0.358738
MC , 100 k			0.358742 ± 0.000718

Table 6: Partial $Z \to b\bar{b}$ decay rate in GeV.

- Benchmark case 2: The process $2f \to 2f$

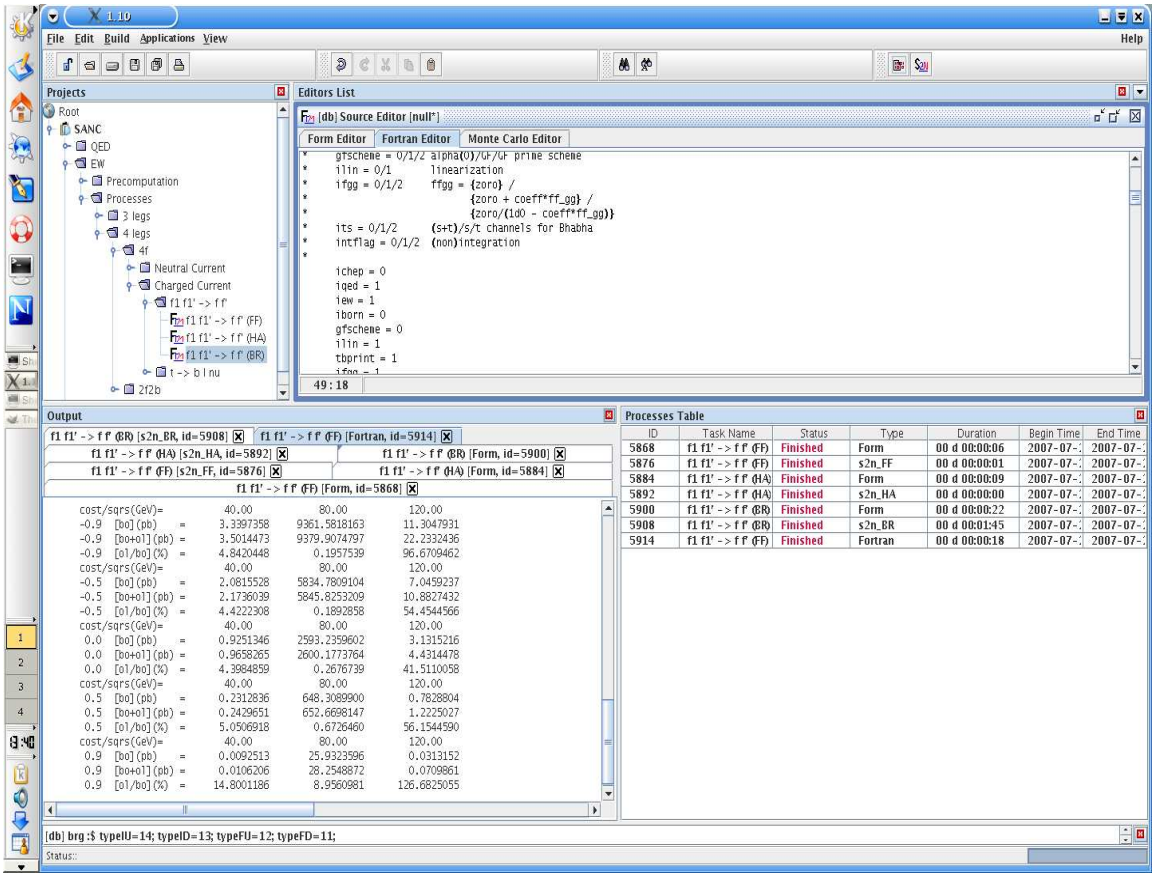

Figure 12: Working status of the SANC windows at the end of calculations for $u\bar{d} \to e^+\nu_e$ process. The output window contains numbers the same as the following Table.

$\cos\theta$		$\sqrt{s}$ GeV 40	80	120
-0.9	Born	3.33973	9361.58	11.3047
	Born + one-loop	3.50144	9379.90	22.2332
-0.5	Born	2.08155	5834.78	7.04592
	Born + one-loop	2.17360	5845.82	10.8827
0.0	Born	0.92513	2593.23	3.13152
	Born + one-loop	0.96582	2600.17	4.43144
0.5	Born	0.23128	648.308	0.78288
	Born + one-loop	0.24296	652.669	1.22250
0.9	Born	0.00925	25.9323	0.03131
	Born + one-loop	0.01062	28.2548	0.07098

Table 7: The differential cross sections in pb for $u\bar{d} \to e^+\nu_e$ for 3 cms energies and 5 cms angles θ.

- Benchmark case 3: $H \to Z f_1 \bar{f}_1$

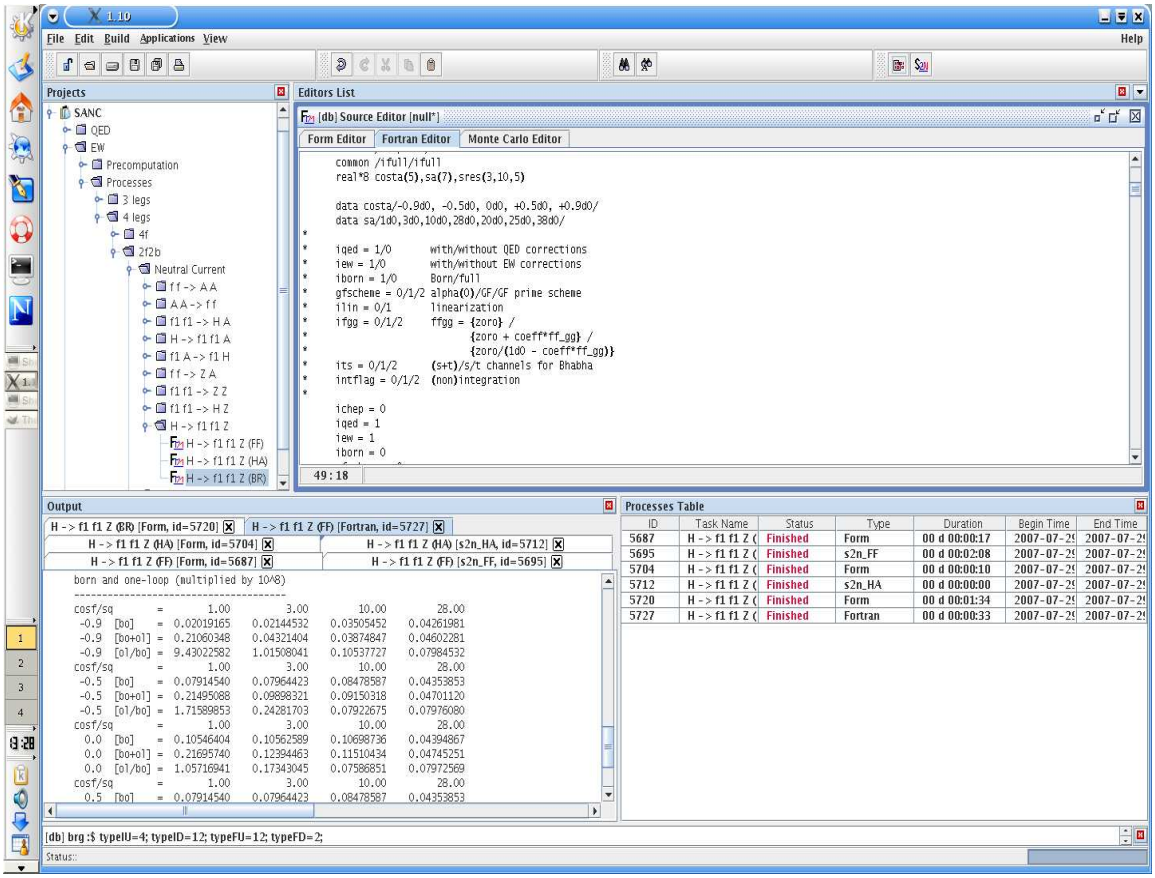

Figure 13: Working status of the SANC windows at the end of calculations for $H \to Z f_1 \bar{f}_1$ decay. The output window contains numbers the same as the following Table.

$H \to e^+e^-Z$					
Part 1, $d^2\Gamma/ds\,d\cos\vartheta_l \cdot 10^8$, GeV^{-1}					
	$\sqrt{s}$, GeV	1	3	10	28
Born		0.02019	0.02144	0.03505	0.04261
1-loop	$\cos\vartheta_l = \pm 0.9$	0.21060	0.04321	0.03874	0.04602
δ		9.43022	1.01508	0.10537	0.07984
Born		0.07914	0.07964	0.08478	0.04353
1-loop	$\cos\vartheta_l = \pm 0.5$	0.21495	0.09898	0.09150	0.04701
δ		1.71589	0.24281	0.07922	0.07976
Born		0.10546	0.10562	0.10698	0.04394
1-loop	$\cos\vartheta_l = 0.0$	0.21695	0.12394	0.11510	0.04745
δ		1.05716	0.17343	0.07586	0.07972

Table 8: The double differential widths for $H \to e^+e^-Z$ decay in α-scheme. First row: the $d^2\Gamma/ds\,d\cos\vartheta_l \cdot 10^8$GeV^{-1} at the Born level; second row: the same but at the 1-loop level; third row: relative correction $\delta = d^2\Gamma^{1-\text{loop}}/d^2\Gamma^{\text{Born}}$. Numerical values are truncated to 6 figures.

References

[1] D. Warding, G. Passarino, L. Kalinovskaya, P. Christova, A. Andonov, S. Bondarenko, and G. Nanava, Project CalcPHEP: Calculus for precision high energy physics, Proceedings of the International Workshop on Computer Algebra and its Application to Physics, CAAP-2001, Dubna 2001. Edited by V.P. Gerdt.

[2] A. Andonov *et al.*, *Nucl. Instrum. Meth.* **A502** (2003) 576–577.

[3] L. V. Kalinovskaya, *Nucl. Instrum. Meth.* **A502** (2003) 581–582.

[4] P. Christova, *Nucl. Instrum. Meth.* **A502** (2003) 578–580.

[5] G. Nanava, *Nucl. Instrum. Meth.* **A502** (2003) 583–585.

[6] D. Bardin and G. Passarino, The standard model in the making: Precision study of the electroweak interactions. Clarendon, 1999. Oxford, UK.

[7] J. A. M. Vermaseren, New features of FORM, [arXiv:math-ph/0010025].

[8] D. Bardin, P. Christova, L. Kalinovskaya, and G. Passarino, *Eur. Phys. J.* **C22** (2001) 99–104.

[9] A. Andonov *et al.*, *Phys. Part. Nucl.* **34** (2003) 577–618.

[10] A. Arbuzov, D. Bardin, and L. Kalinovskaya, Radiative corrections to neutrino deep inelastic scattering revisited, *JHEP* **06** (2005) 078, [arXiv:hep-ph/0407203].

[11] A. Andonov, S. Jadach, G. Nanava, and Z. Was, *Acta Phys. Polon.* **B34** (2003) 2665–2672.

[12] G. Nanava and Z. Was, *Acta Phys. Polon.* **B34** (2003) 4561–4570.

[13] A. Andonov *et al.*, Comput. Phys. Commun. **174** (2006) 481–517.

[14] D. Bardin, S. Bondarenko, L. Kalinovskaya, G. Nanava, L. Rumyantsev and W. von Schlippe, SANCnews: Sector $ffbb$, CPC, "DOI 10.1016/j.cpc.2007.06.006", [arXiv:hep-ph/0506120].

[15] A. Arbuzov *et al.*, Eur. Phys. J. C **46** (2006) 407.

[16] R. Sadykov, et al., in proceedings of "International Workshop of Top Quark Physics", PoS (TOP2006) 036.

[17] A. Arbuzov, D. Bardin, S. Bondarenko, P. Christova, L. Kalinovskaya, G. Nanava, R. Sadykov, and W. von Schlippe, SANCnews: Sector 4f, Charged Current, EPJC, "DOI 10.1140/epjc", [arXiv:hep-ph/0703043].

[18] D. Bardin, S. Bondarenko, L. Kalinovskaya, G. Nanava and L. Rumyantsev, Electroweak radiative corrections to the three channels of the process $f_1\bar{f}_1 HA \to 0$, EPJC, "DOI 10.1140/epjc/s10052-007-0355-y", [arXiv:hep-ph/0702115].

[19] D. Bardin, L. Kalinovskaya, V. Kolesnikov and E. Uglov, Light-by-light scattering in SANC, Talk presented at the International School-Seminar CALC2006, Dubna, 15-25 July 2006, [arXiv:hep-ph/0611188].

[20] A. Andonov, A. Arbuzov, S. Bondarenko, P. Christova, V. Kolesnikov and R. Sadykov, Particles and Nuclei Letters, 6 (2007) 757-771.

[21] D. Bardin, S. Bondarenko, L. Kalinovskaya, G. Nanava and L. Rumyantsev, Electroweak radiative corrections to the three channels of the process $f_1\bar{f}_1 ZA \to 0$, In preparation.

[22] F. Yuasa *et al.*, Prog. Theor. Phys. Suppl. **138** (2000) 18, [arXiv:hep-ph/0007053].

[23] E. Boos *et al.* [CompHEP Collaboration], Nucl. Instrum. Meth. A **534** (2004) 250.

[24] P. Golonka and Z. Was, Eur. Phys. J. C **45** (2006) 97, [arXiv:hep-ph/0506026].

[25] E. Barberio and Z. Was, Comput. Phys. Commun. **79** (1994) 291.

[26] T. Sjostrand, S. Mrenna and P. Skands, JHEP **0605** (2006) 026, [arXiv:hep-ph/0603175].

[27] C. M. Carloni Calame, G. Montagna, O. Nicrosini and M. Treccani, Phys. Rev. D **69** (2004) 037301, [arXiv:hep-ph/0303102].

[28] C. M. Carloni Calame, G. Montagna, O. Nicrosini and M. Treccani, JHEP **0505** (2005) 019, [arXiv:hep-ph/0502218].

[29] C. M. Carloni Calame, G. Montagna, O. Nicrosini and A. Vicini, JHEP **0612** (2006) 016, [arXiv:hep-ph/0609170].

[30] U. Baur, S. Keller and D. Wackeroth, Phys. Rev. D **59** (1999) 013002, [arXiv:hep-ph/9807417].

[31] U. Baur and D. Wackeroth, Phys. Rev. D **70** (2004) 073015, [arXiv:hep-ph/0405191].

[32] U. Baur, S. Keller and W. K. Sakumoto, Phys. Rev. D **57** (1998) 199, [arXiv:hep-ph/9707301].

[33] U. Baur, O. Brein, W. Hollik, C. Schappacher and D. Wackeroth, Phys. Rev. D **65** (2002) 033007.

[34] S. Dittmaier and M. Kramer, Phys. Rev. D **65** (2002) 073007, [arXiv:hep-ph/0109062].

[35] J. Kublbeck, M. Bohm and A. Denner, Comput. Phys. Commun. **60** (1990) 165.

[36] T. Hahn, Comput. Phys. Commun. **140** (2001) 418, [arXiv:hep-ph/0012260].

[37] T. Hahn, Nucl. Phys. Proc. Suppl. **89** (2000) 231, [arXiv:hep-ph/0005029].

[38] T. Hahn and J. I. Illana, Nucl. Phys. Proc. Suppl. **160** (2006) 101, [arXiv:hep-ph/0607049].

[39] G. Belanger, F. Boudjema, J. Fujimoto, T. Ishikawa, T. Kaneko, K. Kato and Y. Shimizu, Phys. Rept. **430** (2006) 117.

[40] T. Hahn and M. Perez-Victoria;http://www.feynarts.de/looptools/).

[41] A. Denner, J. Kublbeck, R. Mertig and M. Bohm, Z. Phys. C **56** (1992) 261.

[42] C. Buttar *et al.*, Les Houches physics at TeV colliders 2005, standard model, QCD, EW, and Higgs working group: Summary report, [arXiv:hep-ph/0604120].

[43] C. E. Gerber *et al.* TeV4LHC-Top and Electroweak Working Group, arXiv:0705.3251 [hep-ph].

[44] A. Djouadi, V. Driesen, W. Hollik and J. Rosiek, Nucl. Phys. B **491** (1997) 68, [arXiv:hep-ph/9609420].

[45] E. Gabrielli, V. A. Ilyin and B. Mele, Phys. Rev. D **56** (1997) 5945; [Erratum-ibid. D **58** (1998) 119902], [arXiv:hep-ph/9702414].

[46] A. Denner and S. Dittmaier, Nucl. Phys. B **398** (1993) 265.

[47] A. B. Arbuzov and R. R. Sadykov, Inverse bremsstrahlung contributions to Drell-Yan like processes, arXiv:0707.0423 [hep-ph].

[48] R. Sadykov and V. Kolesnikov, transparencies, URL: *http://indico.cern.ch/conferenceDisplay.py?confId=6818.*

[49] A. Denner and T. Sack, Nucl. Phys. B **306** (1988) 221,

[50] A. Bredenstein, A. Denner, S. Dittmaier and M. M. Weber, Phys. Rev. D **74** (2006) 013004, [arXiv:hep-ph/0604011].

[51] A. Bredenstein, A. Denner, S. Dittmaier and M. M. Weber, Nucl. Phys. Proc. Suppl. **157** (2006) 63.

[52] I. Boyko, Full simulation study of Higgs bosons produced with SANC generator, the talk at ATLAS Higgs Working Group meeting, 19 April 2006.
URL: *http://indico.cern.ch/conferenceDisplay.py?confId=a058301*.